

Charge transport in melt-dispersed carbon nanotubes

E. K. Hobbie,^{a)} J. Obrzut, and S. B. Kharchenko^{b)}

National Institute of Standards and Technology, Gaithersburg, Maryland 20899

E. A. Grulke

University of Kentucky, Lexington, Kentucky 40506

(Received 8 May 2006; accepted 15 June 2006; published online 27 July 2006)

We investigate the effect of interfacial stabilizer on charge transport in polymer-dispersed carbon nanotubes. Despite mechanical contact, samples with dispersant show poor conductivity, which we attribute to a robust interfacial layer between contacted nanotubes. In comparison, results obtained when nanotubes are mechanically mixed into polymer melts without dispersant show much better conductivity. The difference is striking; at comparable loading, neat melt composites have resistivities five orders of magnitude smaller than those containing interfacial stabilizer. Our results highlight a fundamental issue for the engineering of conducting carbon nanotube composites; dispersion stability will typically be achieved at the expense of conductivity. © 2006 American Institute of Physics. [DOI: 10.1063/1.2221689]

Carbon nanotubes (CNTs) offer great technological promise,¹ particularly in the area of electrically conducting plastics. The large aspect ratios typical of CNTs imply that percolation can be achieved at very low volume fractions, while the intrinsic electrical conductivity of CNTs can be quite large.¹ Despite this potential, efficient dispersion of CNTs in polymeric materials remains a challenging problem that puts limits on processing and production. Surface treatment and interfacial modification in the form of chemical functionalization,² polymer wrapping,³ or surfactants⁴ are all common methods currently used to achieve levels of CNT dispersion in both aqueous and organic environments, but the influence that such stabilization schemes have on charge transport in CNT composites has received limited attention. Here, we investigate the effect of interfacial stabilization on charge transport for polymer dispersed CNTs in the parameter space of concentration, temperature, and shear stress, all of which are relevant to the flow processing of CNT melt composites. Despite mechanical contact and elastic percolation, all samples with interfacial additive show poor conductivity at ambient temperature, which we attribute to a layer of dispersant between contacted nanotubes. Electrical conductivity in these samples is enhanced at elevated temperatures—reflecting the inherent semiconducting nature of the nanotubes—but interfacial charge transport between tubes remains weak, consistent with a robust coating. In comparison, results obtained when comparable nanotubes are mechanically dispersed in polymer melts without additives show much better conductivity. The difference is striking; at the same CNT loading and temperature, neat composites have electrical conductivities five orders of magnitude larger than “stabilized” composites. Our results highlight a fundamental dilemma for engineering CNT materials; dispersion stability will typically be achieved at the expense of conductivity.

Multiwalled carbon nanotubes (MWNTs) were grown via chemical vapor deposition (CVD).⁵ Scanning-electron microscopy (SEM) gave a mean diameter d of 50 nm and the mean length L was determined optically to be 10 μm , with $L/d \approx 200$. The size distribution is nearly log normal with a polydispersity index of 2. The MWNTs were suspended in low-molecular-mass polyisobutylene (PIB) melts using a polymeric dispersant as described elsewhere.⁶ Data are presented for an elastic fluid ($M_w=800$ g/mol with an additional 0.1% at $M_w=4.7 \times 10^6$ g/mol, with a shear viscosity η_s of 10 Pa s, and a first normal stress difference of 5 Pa at a shear rate of 5 s^{-1}) and a Newtonian fluid ($M_w=500$ g/mol and $\eta_s=0.5$ Pa s), denoted m1 and m2, respectively. Suspensions were prepared at 0.025%–10% MWNT by mass with $6 < cL^3 < 2500$ and $0.03 < cL^2d < 15$, where c is the number of nanotubes per unit volume. We compare measurements on these PIB melt composite samples with those obtained for MWNTs of the same type from the same source⁵ melt-mixed at 200 °C into commercial polypropylene (PP) resin ($M_w=4.7 \times 10^6$ g/mol) without the use of any surfactant or dispersant, where η_s is sufficiently large that shearing forces alone can mechanically disperse MWNTs of this length and diameter.⁷ All measurements on PP composites described here were performed at 200 °C, where the PP is fully amorphous, and complications arising from the subtle interaction of polymer crystallinity with the MWNT surface⁸ are thus avoided.

We consider linear shear flow along the x axis with a constant velocity gradient along the y axis and vorticity along the z axis. The shear rate is denoted $\dot{\gamma}$ and we measure electrical conductivity along the y direction. To minimize hysteresis, melts were homogenized at a high $\dot{\gamma}$ and subjected to a damped oscillatory shear flow prior to measurement. The complex linear-viscoelastic shear modulus, $G^*(\omega)=G'(\omega)+iG''(\omega)$, where ω is the angular frequency, was measured in a controlled-strain cone-and-plate rheometer. Measurements of the complex electrical impedance, $Z^*(\omega)=Z'(\omega)+iZ''(\omega)$, at varied nanotube composition (ϕ)

^{a)}Electronic mail: erik.hobbie@nist.gov

^{b)}Present address: Masco Corporation, Operational and Technological Services, Research and Development, Taylor, MI 48180.

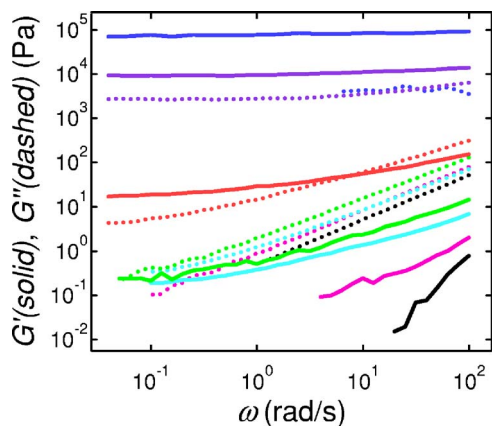


FIG. 1. Complex shear modulus as a function of ω at different ϕ for the suspension m2 at 0% (black), 0.4% (pink), 0.85% (light blue), 1.7% (green), 3% (red), 6% (purple), and 10% (dark blue) MWNT by mass ($T=25^\circ\text{C}$).

were performed as a function of temperature (T) and $\dot{\gamma}$ in a controlled-strain parallel-plate flow cell⁷ that simultaneously recorded the shear viscosity η . Additionally, $Z^*(\omega)$ was measured as a function of T at different ϕ in thick (200 μm) film geometries for quiescent (unsheared) melts. Details of the sample geometry were used to convert $Z^*(\omega)$ to complex conductivity σ^* or resistivity, $\rho^*=(\sigma^*)^{-1}$.

The complex linear-viscoelastic modulus as a function of ω is shown in Fig. 1 for quiescent PIB suspensions at ambient temperature (25°C) at varied ϕ , demonstrating the emergence of an elastic MWNT network with increasing nanotube concentration. Analogous behavior is observed in the melt MWNT-PP dispersions.⁷ For the MWNTs of interest, the overlap concentration—where cL^3 is of order 1 and the nanotubes start to become mechanically entangled—is around 0.005% by mass. Our measurements start at 0.4% MWNT by mass, where a crossover to a low-frequency plateau in the viscoelastic shear modulus is already evident. The application of steady shear flow will destroy this elastic network. With the exception of the high-shear state in which the nanotubes are fully dispersed and aligned along the direction of flow, the MWNTs are in mechanical contact due to aggregation in the presence of strong attractive interactions.⁶

Figure 2 shows $\sigma^*(\omega)$ and $\rho^*(\omega)$ as a function of $\dot{\gamma}$ and quench time for 3% m2 at ambient T (25°C). The response is predominantly that of a dielectric, with $\text{Im}(\sigma^*) \gg \text{Re}(\sigma^*)$ and $\text{Im}(\sigma^*) \propto \omega$, where the linear behavior reflects the capacitive reactance. The growth of aggregate domains under weak shear as a function of time⁶ is evident in the evolution of $\eta(t)$ [inset, Fig. 2(b)] which increases as the aggregates form and coarsen. Associated with this increase in viscosity is a slight decrease in resistivity reflecting aggregation of the MWNTs and a subsequent increase in the dielectric constant of the sample [Fig. 2(b)]. No change is seen in the real part of ρ^* , which remains small. From the data shown in Fig. 2, we deduce that the evolution from elastic MWNT network to isolated MWNT aggregates has very little influence on the sample conductivity. One might expect that the phase-separated MWNTs would behave as a dielectric composite with conducting inclusions, since they can form aggregates physically isolated from one another. The observation that

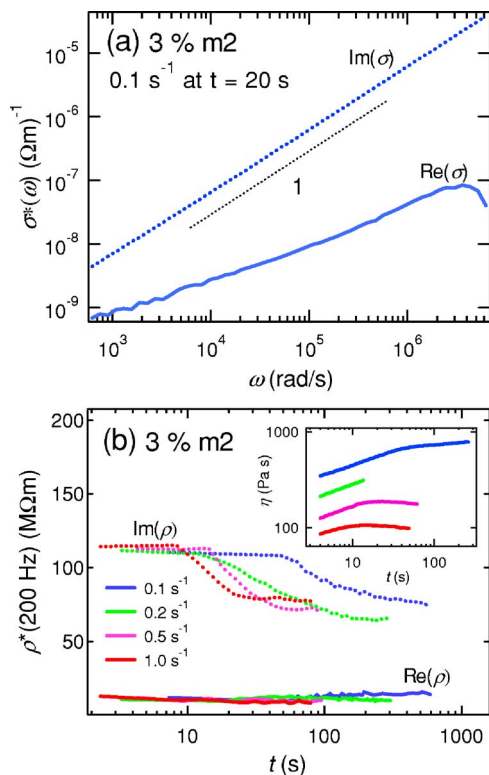


FIG. 2. (a) $\sigma^*(\omega)$ for a 3% m2 suspension 20 s after the inception of slow steady shear and (b) ρ^* at 200 Hz as a function of time for different $\dot{\gamma}$, where the inset shows the simultaneously measured temporal evolution of η . The dashed line (a) shows linear behavior ($T=25^\circ\text{C}$).

the quiescent, mechanically percolated nanotubes have a similar response [as seen in the $t \rightarrow 0$ limit for the data in Fig. 2(b)] is somewhat surprising, however, and suggests that the MWNTs in PIB experience mechanical contact *without* the intimate physical contact needed for interfacial charge transport.

The effect of heating quiescent samples is shown in Fig. 3, which also compares the conductivity for the two different

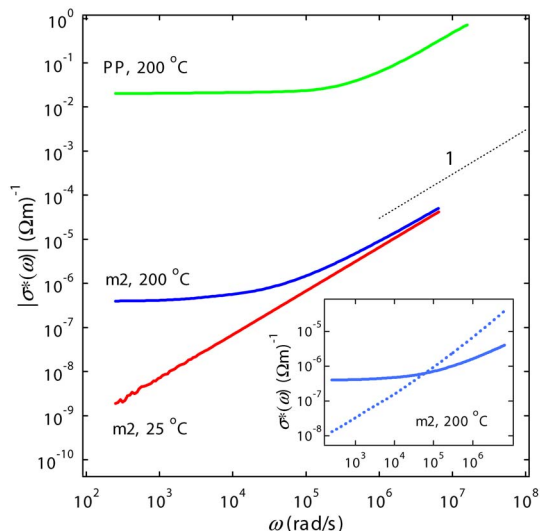


FIG. 3. The effect of heating on a quiescent 200 μm thick 3% m2 sample, where the conductivity of 2.5% neat MWNTs melt mixed in PP at 200°C is shown for comparison and the inset shows the real (solid) and imaginary (dashed) parts of the complex conductivity for m2 at 200°C .

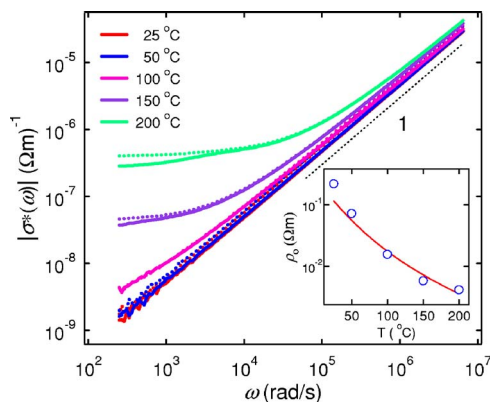


FIG. 4. Effect of heating and annealing on conductivity for a 200 μm film of 0.8% m1, where the inset compares single-MWNT resistivity data from Ref. 7 with our measured ω_c^{-1} (open circles). Measurements during heating (solid) are compared with measurements during cooling after annealing at 200 $^{\circ}\text{C}$ for 10 h (dashed).

types of composite, both with and without dispersant. For m2 at 25 $^{\circ}\text{C}$, the response of the quiescent elastic network is that of a dielectric as described in the previous paragraph. Melt crystallinity of the PP complicates the interpretation of analogous room temperature measurements for the PP-MWNT composites. At elevated T , the response of both samples shows a well-defined frequency, ω_c , marking a crossover from semiconducting to dielectric behavior. Above ω_c , the response is dominated by the imaginary part of σ^* , which grows linearly with ω . Below ω_c , the real part dominates with a low-frequency plateau. The application of steady shear disrupts this low-frequency plateau by destroying the quiescent MWNT network (data not shown). The difference in low-frequency conductivity between the two MWNT composites at 200 $^{\circ}\text{C}$ is quite striking.

The dependence on thermal history is seen in Fig. 4, which shows the conductivity during heating and again during cooling after annealing at 200 $^{\circ}\text{C}$ for 10 h. By fitting the asymptotic high-frequency response to a linear power law, we obtain a quantitative measure of $\omega_c(T)$. As shown in the inset to Fig. 4, this characteristic frequency can be scaled onto the T dependence of the resistivity ρ_o measured for comparable individual MWNTs,⁹ which suggests that the enhanced high- T conductivity merely reflects the inherent semiconducting nature of the CNTs. We found no difference in conductivity between m1 and m2 at varied MWNT loading, temperature, and shear rate, suggesting that melt elasticity does not affect the dielectric response. Although the response in Fig. 4 could also arise from thermally induced changes in the structure of the polymer dispersant layer, an insensitivity of the dielectric response to changes in thermal history suggests that this is not the dominant factor. We also note that the magnitude of the measured conductivity change mirrors the change expected for individual MWNTs.

The magnitude of ρ^* can be modeled as the sum of two contributions; an inherent or *intrinsic* term, ρ_o , and an “interfacial” term, ρ_i . The PIB melts contain a polysuccinimide dispersant ($M_w \approx 10^4$ g/mol) in 1:1 proportion (by mass) with the MWNTs that coats the nanotubes and weakens attractive interactions. We suggest that a thin layer of this in-

terfacial coating persists between MWNTs in mechanical contact, limiting ρ_i . Using⁹ $\rho_o(200^{\circ}\text{C}) \approx 4 \times 10^{-3} \Omega \text{ m}$, $|\rho| \approx 2.5 \times 10^6 \Omega \text{ m}$ at 100 rad/s and 200 $^{\circ}\text{C}$ (Fig. 4) suggests $\rho_i \approx 2.5 \times 10^6 \Omega \text{ m}$ for the PIB suspensions. In contrast, the data for 2.5% neat MWNTs melt mixed into PP at 200 $^{\circ}\text{C}$ without any dispersant (Fig. 3) suggest $\rho_i \approx 50 \Omega \text{ m}$, roughly five orders of magnitude smaller than the PIB suspensions. Although considerably better than m1 and m2, we note that this is still 10^4 times larger than ρ_o , suggesting that there may be significant room for improvement through engineering the “interphase” of mechanically contacted CNTs. Recent efforts along this line have utilized tunable attractive interactions.¹⁰

In conclusion, we investigate the interplay between dispersion stability and electrical conductivity for melt CNT polymer composites in the parameter spaces of shear rate, composition, and temperature. True dispersion is only seen above a critical shear stress for overcoming nanotube flocculation due to attractive interactions, while in quiescence the homogenized dispersions form an elastic network. Charge transport through this network reflects the semiconducting nature of the MWNTs but is limited by weak interfacial conductivity between mechanically contacted MWNTs. Although interfacial coatings are critical for nanotube dispersion, our results suggest that they significantly limit interfacial conductivity, which we suggest is the most critical factor currently limiting the performance of conducting CNT composites. With the scaled-up synthesis of CNTs and a reduction in their costs, extensive investigations of CNT-filled polymer composites have recently become possible.^{11–14} We hope that the results presented here will serve as a guide for developing new processes that mix, mold, and transport CNTs in polymer melts in a manner that optimizes dispersion, processibility, and conductivity.

¹M. S. Dresselhaus and H. Dai, MRS Bull. **29**, 237 (2004).

²F. Liang, A. K. Sadana, A. Peera, J. Chattopadhyay, Z. Gu, R. H. Hauge, and W. E. Billups, Nano Lett. **4**, 1257 (2004).

³M. Zheng, A. Jagota, E. D. Semke, B. A. Diner, R. S. McLean, S. R. Lustig, R. E. Richardson, and N. G. Tassi, Nat. Mater. **2**, 338 (2003).

⁴H. Wang, W. Zhou, D. L. Ho, K. I. Winey, J. E. Fischer, C. J. Glinka, and E. K. Hobbie, Nano Lett. **4**, 1789 (2004); M. F. Islam, E. Rojas, D. M. Bergey, A. T. Johnson, and A. G. Yodh, *ibid.* **3**, 269 (2003).

⁵R. Andrews, D. Jacques, A. M. Rao, F. Derbyshire, D. Qian, X. Fan, E. C. Dickey, and J. Chen, Chem. Phys. Lett. **303**, 467 (1999).

⁶S. Lin-Gibson, J. A. Pathak, E. A. Grulke, H. Wang, and E. K. Hobbie, Phys. Rev. Lett. **92**, 048302 (2004); D. Fry, B. Langhorst, H. Kim, E. Grulke, H. Wang, and E. K. Hobbie, *ibid.* **95**, 038304 (2005).

⁷S. B. Kharchenko, J. F. Douglas, J. Obrzut, E. A. Grulke, and K. B. Migler, Nat. Mater. **3**, 564 (2004); M. Pasquali, *ibid.* **3**, 509 (2004).

⁸C. Y. Li, L. Li, W. Cai, S. L. Kodjie, and K. K. Tenneti, Adv. Mater. (Weinheim, Ger.) **17**, 1198 (2005).

⁹B. Wei, R. Spolenak, P. Kohler-Redlich, M. Rühle, and E. Arzt, Appl. Phys. Lett. **74**, 3149 (1999).

¹⁰B. Vigolo, C. Coulon, M. Maugey, C. Zakri, and P. Poulin, Science **309**, 920 (2005).

¹¹F. M. Du, J. E. Fischer, and K. I. Winey, J. Polym. Sci., Part B: Polym. Phys. **41**, 3333 (2003).

¹²C. Park, Z. Ounaies, K. A. Watson, R. E. Crooks, J. Smith, Jr., S. E. Lowther, J. W. Connell, E. J. Siochi, J. S. Harrison, and T. L. St. Clair, Chem. Phys. Lett. **364**, 303 (2002).

¹³S. Kumar, T. D. Dang, F. E. Arnold *et al.*, Macromolecules **35**, 9039 (2002).

¹⁴C. A. Mitchell, J. L. Bahr, S. Arepalli, J. M. Tour, and R. Krishnamoorti, Macromolecules **35**, 8825 (2002).